JPE 16-4-20

http://dx.doi.org/10.6113/JPE.2016.16.4.1438
ISSN(Print): 1598-2092 / ISSN(Online): 2093-4718

A Six-Phase CRIM Driving CVT using Blend Modified Recurrent Gegenbauer OPNN Control

Chih-Hong Lin†

†Department of Electrical Engineering, National United University, Miaoli, Taiwan

Abstract

Because the nonlinear and time-varying characteristics of continuously variable transmission (CVT) systems driven by means of a six-phase copper rotor induction motor (CRIM) are unconscious, the control performance obtained for classical linear controllers is disappointing, when compared to more complex, nonlinear control methods. A blend modified recurrent Gegenbauer orthogonal polynomial neural network (OPNN) control system which has the online learning capability to come back to a nonlinear time-varying system, was complied to overcome difficulty in the design of a linear controller for six-phase CRIM driving CVT systems with lumped nonlinear load disturbances. The blend modified recurrent Gegenbauer OPNN control system can carry out examiner control, modified recurrent Gegenbauer OPNN control, and reimbursed control. Additionally, the adaptation law of the online parameters in the modified recurrent Gegenbauer OPNN is established on the Lyapunov stability theorem. The use of an amended artificial bee colony (ABC) optimization technique brought about two optimal learning rates for the parameters, which helped reform convergence. Finally, a comparison of the experimental results of the present study with those of previous studies demonstrates the high control performance of the proposed control scheme.

Key words: Artificial bee colony optimization, Lyapunov stability theorem, Modified recurrent Gegenbauer orthogonal polynomial neural network, Six-phase copper rotor induction motor

I. INTRODUCTION

Six-phase induction motors (IM) can generate a higher torque when compared to conventional three-phase IM. This characteristic makes them convenient in high power and high current applications, such as ship propulsion, aerospace applications, and electric/hybrid vehicles (EV) [1]. A six-phase copper rotor induction motor (CRIM) [2] is chosen as an alternating current (AC) motor driving a continuously variable transmission (CVT) system because it provides lower torque ripple, higher efficiency, and better reliability for its size when compared to single-phase and three-phase aluminum rotor IMs [3]-[8]. However, a simplified model of a CVT system, which is driven by a six-phase CRIM, has not been presented. This research gap, which includes the derived procedures, simplified models and control schemes, provided the motivation for the current study.

A CVT system [2], [9]-[16] may be manipulated at a specific speed while changing the pulleys' radii for achieving torque multiplication, acceleration, and speed. This working profile provides the research motivation for the CVT dynamics and nonlinear control algorithms. A standard proportional integral derivative (PID)-based controller with measurements of the gear ratio has been applied in CVT-based vehicle regulation [11]. This control scheme demonstrates satisfactory performance by using a gain-scheduling with a large set of points. In addition, the design of numerous fuzzy controllers for a CVT hydraulic module has been reported by Kim [12].

Some of the principal advantages of using artificial neural networks (ANNs) are their good learning ability and good performance for the tasks of system identification and control [17]-[20]. However, one of the major drawbacks of the ANNs is to need for a large number of iterations and computationally intensive time for its training. Functional link NNs [21]-[23] have been reported to reduce computational complexity. These functional link NNs [21]-[23] with a reduced computational complexity and faster convergence have been used for executing the identification and control of the nonlinear systems. Recently, some

Manuscript received Nov. 11, 2015; accepted Apr. 9, 2016
Recommended for publication by Associate Editor Shihua Li.
†Corresponding Author: jhlin@nuu.edu.tw
Tel:+886-3-7382464, Fax:+886-3-7382488, National United University
Dept. of Electrical Eng., National United University, Taiwan

Gegenbauer functional expansions [24]-[26] combined with NNs have been proposed. They have been applied to highly nonlinear approximations, identifications, compensations and controls of systems. Gegenbauer polynomial approximation in the presence of the parameter uncertainty characteristics of a two-dimensional airfoil has been reported by Belmehdi [24]. A Gegenbauer NN by means of a weights direct determination method in order to avoid a longer iterative-training procedure for nonlinear system has been proposed by Wu et al. [25]. A feedforward NN with Gegenbauer orthogonal functions through the use of a weights direct determination method has been proposed by Zhang and Li [26]. Because a Gegenbauer NN is a single-layer NN, its computational complexity is considerably lower than that of a multilayer perceptron. However, some Gegenbauer functional expansion feedforward NNs [24]-[26] can be used for static function approximations. However, they cannot effectively identify complex dynamic systems due to the absence of an appropriate feedback loop.

Recurrent NNs, which have been used for modeling nonlinear systems and for the dynamic control of systems [27]-[31] have received considerable attention because of their structural advantages. Because of their high computational complexity, these NNs can effectively identify and control complex dynamic systems. Therefore, to reduce the computational complexity and to enhance the identification ability of high-order nonlinear systems, the modified recurrent Gegenbauer OPNN [2] , which offers more advantages than the Gegenbauer OPNN [24]-[26] including better performance, higher accuracy and dynamic robustness, was proposed for controlling a six-phase CRIM driving CVT system with nonlinear and time-varying characteristics in this paper.

Karaboga [32] makes use of the artificial bee colony (ABC) optimization algorithm for solving numerical methods in optimization problems. This algorithm was further advanced by Karaboga and Basturk [33]-[35]. It is a popular swarm intelligence technique based on the intelligent foraging behavior of honey bees. It is a very simple and robust population based stochastic optimization algorithm. In ABC optimization algorithms, a colony of artificial bees contains three groups of bees: worker bees, onlookers and scouts. A bee waiting in the dance area to make a decision to choose a food source is called an onlooker and the one going to the food source visited by the onlooker is called a worker bee. The other kind of bee is a scout bee that carries out random searches for discovering new sources. In a robust search process, exploration and exploitation processes must be carried out together. In the ABC optimization algorithm, while onlookers and worker bees carry out the exploitation process in the search space, the scouts control the exploration process. However, the ABC optimization algorithm is good at exploration but poor at exploitation. In addition, its convergence speed is slow in some cases [36], [37]. Therefore, to further improve the performance of ABC optimization, some modified ABC optimizations inspired by using the Grenade explosion method [38], [39] and the Bisection explosion method [40], [41] were proposed. However, since the ABC optimization method possess a slow convergence, the amended ABC optimization [2] with an inertia weight is proposed to search for two optimal learning rates of the weights in the modified recurrent Gegenbauer OPNN. This is done in order to obtain faster convergence and a better learning rate in this study.

In this study, because CVT systems [2], [9]-[16], [42]-[45] possess nonlinear dynamics and uncertainties, the blend modified recurrent Gegenbauer OPNN control system using an amended ABC optimization [2] is proposed for controlling a six-phase CRIM driving CVT system. The blend modified recurrent Gegenbauer OPNN control system using an amended ABC optimization [2] has a good generalization ability and a fast learning capability. The proposed control scheme can adapt to any change in the system. The blend modified recurrent Gegenbauer OPNN control system using an amended ABC optimization [2], which is composed of the examiner control, the modified recurrent Gegenbauer OPNN control with an adaptation law, and the reimbursed control with an estimation law, is applied in the six-phase CRIM driving CVT system. According to the Lyapunov stability and gradient descent method, the adaptation law of the modified recurrent Gegenbauer OPNN is derived for online training of the parameters. Therefore, the modified recurrent Gegenbauer OPNN can react to the system's nonlinear and time-varying behaviors by the online learning procedure under lumped nonlinear external disturbances and parameter variations. Furthermore, two optimal learning rates for the modified recurrent Gegenbauer OPNN using an amended ABC optimization method [2] are proposed to achieve a better convergence. The experimental results shown obtained using the proposed blend modified recurrent Gegenbauer OPNN control scheme and the amended ABC optimization [2] are shown to achieve better control performances.

This paper is organized as follows. The system structure of the six-phase CRIM driving CVT system is reviewed in Section II. The design methods of a blend modified recurrent Gegenbauer OPNN control system and an amended ABC optimization [2] are presented in Section III. Experimental results are illustrated in Section IV. Some conclusions are given in Section V.

II. Configuration of Six-Phase CRIM Driving CVT System

In order to reduce the complexity of the system, the rotation dynamic equations in the primary drive shaft and the

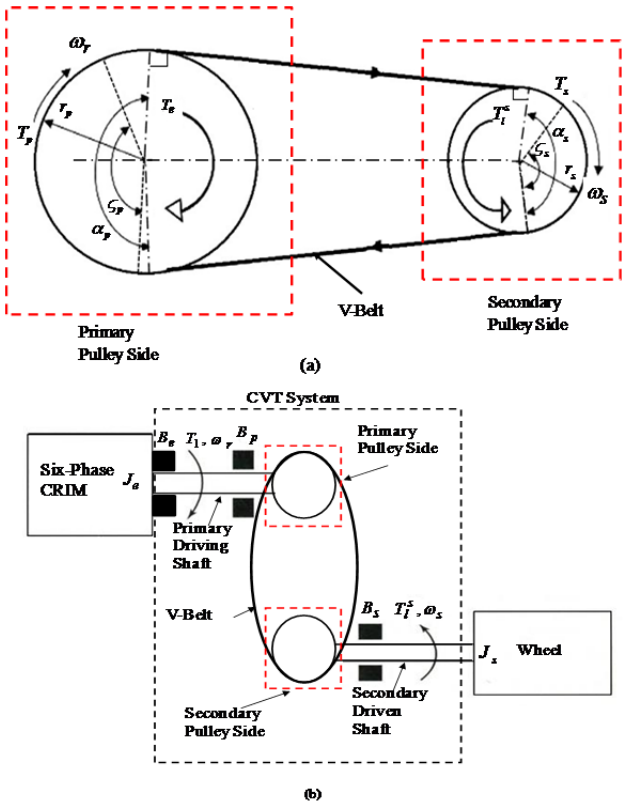

Fig. 1. Schematic of the CVT system driven by six-phase CRIM. (a) Geometrical description of the CVT system. (b) Geometrical description of the six-phase CRIM-wheel connection via the CVT system.

secondary drive shaft of the CVT, shown in Fig. 1, can be simplified as [2], [9]-[16], [42]-[45]:

$$T_s = J_s\dot{\omega}_s + B_s\omega_s + T_l^s(T_a, \Delta T_p, F_l, \upsilon_a, \tau_a, \omega_s^2) \quad (1)$$

$$J_p\dot{\omega}_r + B_p\omega_r + T_p = T_e \quad (2)$$

in which $T_l^s(T_a, \Delta T_p, F_l, \upsilon_a, \tau_a, \omega_s^2)$ [9]-[16] is the lumped nonlinear disturbance in the secondary pulley side with the wheel; $T_p = \sigma_s\omega_s T_s/\omega_r$ is the output torque in the primary pulley shaft; T_s is the output torque in the secondary pulley shaft; T_e is the drive torque in the secondary pulley shaft; σ_s is the conversion ratio; ΔT_p is the parameter variation; υ_a is the rolling resistance; τ_a is the wind resistance; F_l is a braking force; B_p and B_s represent the equivalent viscous frictional coefficients of the primary pulley shaft and the secondary pulley shaft, respectively; J_p and J_s are the equivalent inertia of the primary pulley shaft and the secondary pulley shaft including a wheel, respectively; and ω_r and ω_s are the speeds of the primary pulley shaft and the secondary pulley shaft, respectively.

Using the speed conversion ratio and the sliding conversion ratio [9]-[16], the resultant dynamic equation of a CVT system driven by a six-phase CRIM from (1) and (2) can be simplified as [9]-[16]:

$$J_r\dot{\omega}_r + B_r\omega_r + T_l(T_{ar}, \Delta T_{pr}, F_l, \upsilon_{ar}, \tau_{ar}, \omega_r^2) = T_1 \quad (3)$$

where $T_1 = \sigma_r T_e$ is the air-gap torque of a CVT system via the conversion ratio; σ_r is the conversion ratio; $T_l(T_{ar}, \Delta T_{pr}, F_{lr}, \upsilon_{ar}, \tau_{ar}, \omega_r^2) = T_l(T_{ar} + \Delta T_{pr} + T_{un})$ [9]-[16] is the resultant lumped nonlinear external disturbance with parameter variations; T_{ar} is the resultant fixed load torque; $\Delta T_{pr} = \Delta J_r\dot{\omega}_r + \Delta B_r\omega_r$ is the resultant parameter variation; υ_{ar} is the resultant rolling resistance; τ_{ar} is the resultant wind resistance; F_{lr} is the resultant braking force; $T_{un} = F_{lr} + \upsilon_{ar} + \tau_{ar}\omega_r^2$ is the resultant unknown nonlinear load torque; $B_r = B_p + B_e$ is the resultant viscous frictional coefficient; $J_r = J_p + J_e$ is the resultant moment of inertia; and J_e and B_e represent the moment of inertia and the viscous frictional coefficients of the six-phase CRIM, respectively.

The *d*-*q* axes voltage equations of a six-phase CRIM in the synchronously reference frame can be described as follows [2]-[8]:

$$v_{q1}^e = r_s i_{q1}^e + \omega_e(L_{ss} i_{d1}^e + L_M i_{dr}^e) + d(L_{ss} i_{q1}^e + L_M i_{qr}^e)/dt \quad (4)$$

$$v_{d1}^e = r_s i_{d1}^e - \omega_e(L_{ss} i_{q1}^e + L_M i_{qr}^e) + d(L_{ss} i_{d1}^e + L_M i_{dr}^e)/dt \quad (5)$$

$$v_{q2}^e = r_s i_{q2}^e + d(L_{ss} i_{q2}^e)/dt \quad (6)$$

$$v_{d2}^e = r_s i_{d2}^e + d(L_{ss} i_{d2}^e)/dt \quad (7)$$

$$0 = r'_r i_{qr}^e + (\omega_e - \omega_r)(L_{ss} i_{dr}^e + L_M i_{d1}^e) + d(L_{rr} i_{qr}^e + L_M i_{q1}^e)/dt \quad (8)$$

$$0 = r'_r i_{dr}^e - (\omega_e - \omega_r)(L_{rr} i_{qr}^e + L_M i_{q1}^e) + d(L_{ss} i_{dr}^e + L_M i_{d1}^e)/dt \quad (9)$$

where $L_{ss} = L_{ls} + 3L_{ms}$, $L_{rr} = L_{lr} + 3L_{ms}$, and $L_M = 3L_{ms}$.

The air-gap torque T_1 of a CVT system driven by a six-phase CRIM can be represented as:

$$T_1 = 3P_1 L_M [\lambda_{dr}^e i_{q1}^e - \lambda_{qr}^e i_{d1}^e]/(4L_{rr}) \quad (10)$$

in which v_{q1}^e, v_{d1}^e and v_{q2}^e, v_{d2}^e are the *d*-axis and *q*-axis voltages; i_{q1}^e, i_{d1}^e and i_{q2}^e, i_{d2}^e are the *d*-axis and *q*-axis currents; L_{ss}, L_{rr}, and L_M are the self-inductance of the stator, the self-inductance of the rotor, and the mutual inductance between the stator and the rotor, respectively; r_s and r'_r are the stator resistance and the rotor resistance; λ_{dr}^e and λ_{qr}^e are the *d*-axis and *q*-axis flux linkages; and

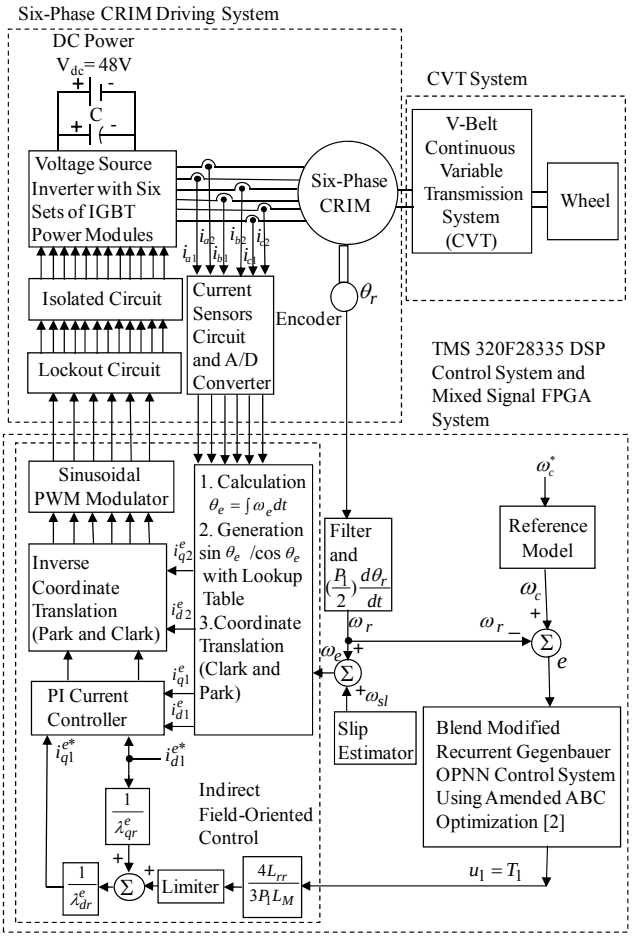

Fig. 2 Block diagram of a six-phase CRIM driving CVT system.

P_1 is the number of poles.

A block diagram of the six-phase CRIM driving CVT system is shown in Fig. 2. The whole system of the six-phase CRIM driving CVT system can be indicated as follows: an indirect-field-oriented control with a current proportional-integral (PI) control, a sinusoidal pulse width modulation (PWM) control modulator, an interlock circuit, an isolated circuit, a voltage source inverter with six sets of insulated-gate bipolar transistor (IGBT) power modules and a speed control. The PI current loop controller is the current loop tracking controller. In order to attain a good dynamic response, all of the gains for a well-known PI current controller are listed as follows: $k_{pc} = 14.5$ and $k_{ic} = k_{pc}/T_{ic} = 5.2$ through some heuristic knowledge [46-48]. The indirect field-oriented control consists of a coordinate transformation, a $\sin\theta_e / \cos\theta_e$ generation with lookup table generation and a PI current control. A TMS320F28335 digital-signal-processor (DSP) control system with a mix signal field-programmable-gate-array (FPGA) system manufactured by the Microcontroller Corporation of Taiwan was used to implement the indirect field-oriented control and the speed control. The six-phase CRIM driving CVT system was operated under lumped external disturbances and with nonlinear uncertainties.

III. Blend Modified Recurrent Gegenbauer OPNN Control System

The dynamic equation of a CVT system driven by the six-phase CRIM from (3) can be rewritten as:

$$\dot{\omega}_r = A_1\omega_r + C_1T_l(T_{ar} + \Delta T_{pr} + T_{un}) + B_1u_1 \tag{11}$$

Then, the tracking error e of the speed can be represented as:

$$e = \omega_c - \omega_r \tag{12}$$

in which $u_1 = T_1$ is the control torque of the CVT system driven by a six-phase CRIM. $A_1 = -B_r/J_r$, $B_1 = 1/J_r$ and $C_1 = -1/J_r$ are three known constants. ω_c represents the desired command rotor speed. All of the parameters are assumed to be bounded and well known under the occurrence of uncertainties. Then, the ideal control law can be designed as:

$$u_1^* = [\dot{\omega}_c + k_1e - A_1\omega_r - C_1T_l(T_{ar} + \Delta T_{pr} + T_{un})]/B_1 \tag{13}$$

Substituting (13) with $u_1^* = u_1$ into (11) and using (12), the dynamic equation of the error can be obtained as:

$$\dot{e} + k_1e = 0 \tag{14}$$

in which k_1 is a positive constant. The system state can track a desired trajectory when $e(t) \to 0$ as $t \to \infty$ in (14).

Because unknown uncertainties are difficult to measure, the control law u_1 of the blend modified recurrent Gegenbauer OPNN control system shown in Fig. 3 can be designed as:

$$u_1 = u_{co} + u_{rm} + u_{r1} \tag{15}$$

where u_{co} is the examiner control system; u_{rm} is the modified recurrent Gegenbauer OPNN controller; and u_{r1} is the reimbursed controller. The examiner control system u_{co} is designed so that the state of the controlled system is stabilized around a predetermined bound region. Due to the excessive and chattering control effort induced by the examiner controller u_{co}, the modified recurrent Gegenbauer OPNN controller u_{rm} and the reimbursed controller u_{r1} are introduced to reduce and smooth the control effort when the system state is inside a predefined bound region. The modified recurrent Gegenbauer OPNN controller u_{rm} is the main tracking controller, which used to mimic an ideal control law u_1^*. The reimbursed controller u_{r1} is designed to compensate the difference between the ideal control law u_1^* and the modified recurrent Gegenbauer OPNN controller u_{rm}. Since the examiner control system u_{co} caused the excessive and chattering effort, the modified recurrent

Gegenbauer OPNN controller u_{rm} and the reimbursed controller u_{r1} are proposed to reduce and smooth the control effort when the system states are inside a predetermined bound area. When the modified recurrent Gegenbauer OPNN approximation properties cannot be ensured, the examiner control system u_{co} is able to take action. The design of the blend modified recurrent Gegenbauer OPNN control system is necessary for the divergence of the states to pull the states back to a predetermined bound region and guarantee the stability of the system. The control law u_1 of the blend modified recurrent Gegenbauer OPNN control system uniformly approximates the ideal control law u_1^* inside the bound region.

A. Design of the Examiner Control System

First, the error equation from (11) to (15) can be obtained as:

$$\dot{e} = -k_1 e + [u_1^* - u_{co} - u_{rm} - u_{r1}]B_1 \tag{16}$$

Then the Lyapunov function candidate is defined as:

$$S_1 = e^2 / 2 \tag{17}$$

Differentiating (17) with respect to time and using (16) results in:

$$\begin{aligned} \dot{S}_1 &= e\dot{e} = e[-k_1 e + B_1(u_1^* - u_{co} - u_{rm} - u_{r1})] \\ &\le -k_1 e^2 + |eB_1| \cdot \left(|u_1^*| + |u_{rm} + u_{r1}| \right) - eB_1 u_{co} \end{aligned} \tag{18}$$

To satisfy $\dot{S}_1 \le 0$, the examiner control system u_{co} is designed as:

$$\begin{aligned} u_{co} &= I_{co}\, \mathrm{sgn}(eB_1) \cdot \\ &[|u_{rm} + u_{r1}| + D_1(\omega_r) + D_2 + |\dot{\omega}_c| + |k_1 e|] / B_1 \end{aligned} \tag{19}$$

where $\mathrm{sgn}(\cdot)$ is a sign function. In addition, $A_1\omega_r \le D_1(\omega_r)$, and $C_1 T_l (T_{ar} + \Delta T_{pr} + T_{un}) \le D_2$. Then the operator index can be denoted as:

$$I_{co} = \begin{cases} I_{co} = 1, & if \quad S_1 \ge \overline{H} \\ I_{co} = 0 & if \quad S_1 < \overline{H} \end{cases} \tag{20}$$

in which $\overline{H}$ is the boundary constant specified by the designer. The parameter value of $\overline{H}$ in this study is unity according to the system character. Substituting (19) into (18) and using (20) with $I_{co} = 1$ results in:

$$\begin{aligned} \dot{S}_1 &\le -k_1 e^2 + |eB_1| \cdot \left(|u_1^*| + |u_{rm} + u_{r1}| \right) - eB_1 u_{co} \\ &\le -k_1 e^2 + |eB_1| \{ [A_1\omega_r + C_1 T_l (T_{ar} + \Delta T_{pr} + T_{un})] / B_1 \\ &\quad - [D_1(\omega_r) + D_2] / B_1 \} \\ &\le -k_1 e^2 \le 0 \end{aligned} \tag{21}$$

Using the examiner control system u_{co}, as shown in (19), the inequality $\dot{S}_1 < 0$ can be obtained for a nonzero value of the tracking error vector e when $S_1 > \overline{H}$. With the results from (21), the examiner control system u_{co} is able to drive the tracking error to zero without using the modified recurrent Gegenbauer OPNN controller u_{rm} or the reimbursed controller u_{r1}. However, owing to the selection of the bounds $D_1(\omega_r)$ D_2 and the sign function, the examiner control system u_{co} can result in excessive and chattering control effort. Therefore, the modified recurrent Gegenbauer OPNN controller u_{rm} and the reimbursed controller u_{r1} are designed to overcome this drawback. The modified recurrent Gegenbauer OPNN controller u_{rm} is used to imitate the ideal control law u_1^*. Then the reimbursed controller u_{r1} is posed to compensate the difference between the ideal control law u_1^* and the modified recurrent Gegenbauer OPNN controller u_{rm}.

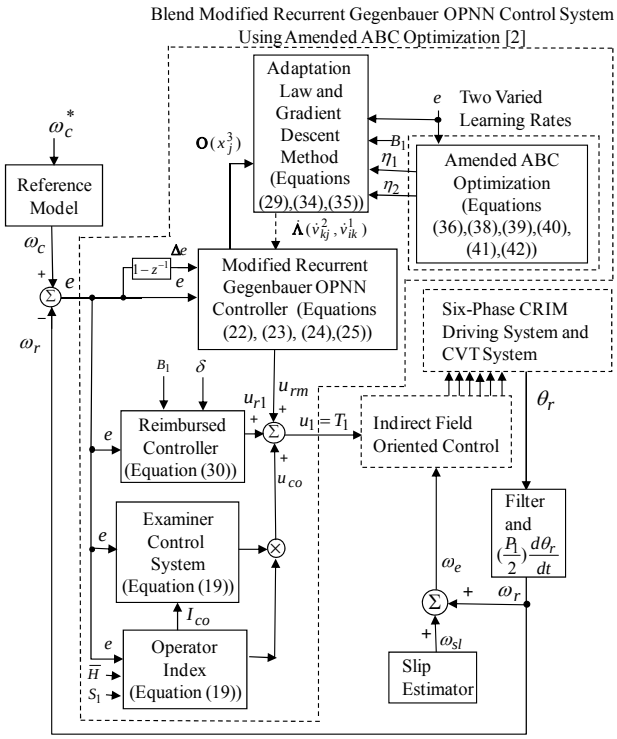

Fig. 3. Block diagram of the blend modified recurrent Gegenbauer Gegenbauer OPNN control system and amended ABC optimization [2].

B. Design of the Modified Recurrent Gegenbauer OPNN Controller

Second, the modified recurrent Gegenbauer OPNN controller u_{rm} is equal to $y_k^3(N)$ as the output value of the modified recurrent Gegenbauer OPNN. In this case, the input values and the output values of the modified recurrent Gegenbauer OPNN with a three-layer structure (an input

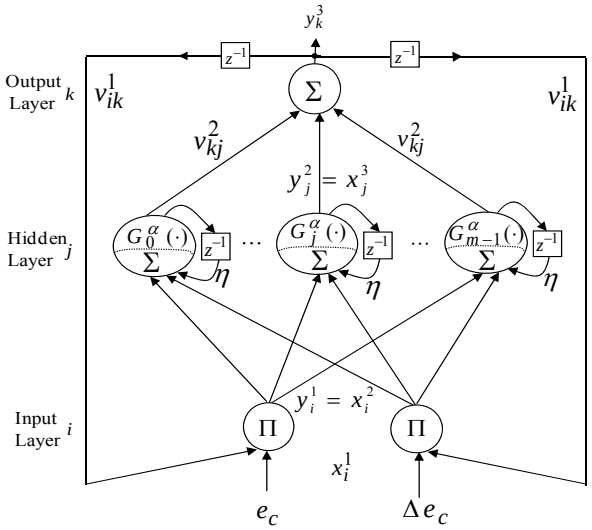

Fig. 4. Structure of the three-layer modified recurrent Gegenbauer OPNN.

layer, a hidden layer and an output layer), as shown in Fig. 4, can be expressed as:

$$y_i^1 = f_i^1(\prod_k x_i^1(N) v_{ik}^1 y_k^3(N-1)), \quad i = 1, 2 \tag{22}$$

$$y_j^2 = G_j^\sigma(\sum_{i=1}^{2} y_i^1(N) + \beta\ y_j^2(N-1)),\ j = 0, 1, \cdots, m-1 \tag{23}$$

$$y_k^3 = f_k^3(\sum_{j=0}^{m-1} v_{kj}^2 y_j^2(N)), \quad k = 1 \tag{24}$$

where $x_1^1 = \omega_c - \omega_r = e$ and $x_2^1 = e(1-z^{-1}) = \Delta e$ are the speed error and the speed error change, respectively. v_{ik}^1 and v_{kj}^2 are the recurrent weight and the connective weight. N denotes the number of iterations. The Gegenbauer orthogonal polynomial [24-26] $G_n^\sigma(x)$ is the argument of the polynomials with $-1 < x < 1$; where σ and n are the number of the order and the order of the expansion, respectively. m is the number of nodes. β is the self-connecting feedback gain of the hidden layer between 0 and 1. The zero, first and second order Gegenbauer orthogonal polynomials are given by $G_0^\sigma(x) = 1$, $G_1^\sigma(x) = 2\sigma x$ and $G_2^\sigma(x) = 2x^2(\sigma+1)\sigma - \sigma$, respectively. The higher order Gegenbauer orthogonal polynomials may be generated by the recursive formula given by $G_n^\sigma(x) = [2(n+\sigma-1)xG_{n-1}^\sigma(x) - (n+2\sigma+2)G_{n-2}^\sigma(x)]/n$. f_i^1, f_k^3 is the activation function which is selected as a linear function. The output $u_{rm} = y_k^3(N)$ of the modified recurrent Gegenbauer OPNN controller can be denoted as:

$$u_{rm} = y_k^3(N) = \begin{bmatrix} v_{10}^2 & \cdots & v_{1,m-1}^2 \end{bmatrix} \begin{bmatrix} x_0^3 & \cdots & x_{m-1}^3 \end{bmatrix}^T = \mathbf{\Lambda}^T \mathbf{O} \tag{25}$$

where $\mathbf{\Lambda} = \begin{bmatrix} v_{10}^2 & \cdots & v_{1,m-1}^2 \end{bmatrix}^T$ are the adjustable weight parameter vectors of the modified recurrent Gegenbauer OPNN, and $\mathbf{O} = \begin{bmatrix} x_0^3 & \cdots & x_{m-1}^3 \end{bmatrix}^T$ are the input parameter vectors in the output layer, in which x_j^3 is determined by the selected Gegenbauer orthogonal polynomials and $0 \le x_j^3 \le 1$.

C. Design of the Reimbursed Controller and the Adaptation Law

Third, to develop the reimbursed controller u_{r1}, the approximation error ρ can be defined as:

$$\rho = u_1^* - u_{rm}^* = u_1^* - (\mathbf{\Lambda}^*)^T \mathbf{O} \tag{26}$$

in which $\mathbf{\Lambda}^*$ is the ideal weight vector to reach the minimum approximation error. It is assumed that the absolute value of ρ is less than a small positive number δ, i.e., $|\rho| < \delta$. By substituting (25) and (26) into (16), the error dynamic equation from (16) can be rewritten as:

$$\begin{aligned} \dot{e} &= -k_1 e + [u_1^* - u_{co} - u_{rm} - u_{r1}]B_1 \\ &= -k_1 e + [(u_1^* - u_{rm}^* + u_{rm}^* - u_{rm}) - u_{co} - u_{r1}]B_1 \\ &= -k_1 e + [\rho + (\mathbf{\Lambda}^* - \mathbf{\Lambda})^T \mathbf{O} - u_{r1} - u_{co}]B_1 \end{aligned} \tag{27}$$

Then, the Lyapunov function is selected as:

$$S_2(t) = e^2/2 + (\mathbf{\Lambda}^* - \mathbf{\Lambda})^T (\mathbf{\Lambda}^* - \mathbf{\Lambda})/(2\eta_1) \tag{28}$$

Taking derivative of (28) and using (27), then (28) can be rewritten as:

$$\begin{aligned} \dot{S}2(t) = \{&-k_1 e^2 + [\rho - u_{r1} - u_{co}]B_1 e \\ &+ (\mathbf{\Lambda}^* - \mathbf{\Lambda})^T \mathbf{O}\, B_1 e - (\mathbf{\Lambda}^* - \mathbf{\Lambda})^T \dot{\mathbf{\Lambda}}/\eta_1 \end{aligned} \tag{29}$$

Then the adaptation law $\dot{\mathbf{\Lambda}}$ and the reimbursed controller u_{r1} can be designed as follows:

$$\dot{\mathbf{\Lambda}} = \eta_1 \mathbf{O}\, B_1 e \tag{30}$$

$$u_{r1} = \delta\, \mathrm{sgn}(B_1 e) \tag{31}$$

in which η_1 and δ are the learning rate and the gain, respectively. Substituting (19) with I_{co}=0, (30) and (31) into (29), then (29) can be represented as:

$$\dot{S}_2(t) \le -k_1 e^2 + \{|\rho| - \delta\}|B_1 e| \le -k_1 e^2 \le 0 \tag{32}$$

From (32), $\dot{S}_2(t)$ is a negative semi-definite, i.e. $S_2(t) \le S_2(0)$. This implies that e and $(\mathbf{\Lambda}^* - \mathbf{\Lambda})$ are bounded. In addition, the function $\varepsilon(t)$ is defined as $\varepsilon(t) = -\dot{S}_2(t) = k_1 e^2$, and it is a uniformly continuous function. It is denoted that $\lim_{t\to\infty} \varepsilon(t) = 0$ by using Barbalat's lemma [49], [50]. Then $e(t) \to 0$ as $t \to \infty$.

D. Online Parameter Training Methodology

Finally, the online parameter training methodology of the modified recurrent Gegenbauer OPNN can be derived and trained effectively according to the Lyapunov stability theorem. The parameter of the adaptation law $\dot{\Lambda}$ shown in (30) can be rewritten as:

$$\dot{v}_{kj}^{2} = \eta_1 \, y_j^2 \, B_1 e \tag{33}$$

Then the cost function is defined as:

$$R_1 = e^2 / 2 \tag{34}$$

The adaptation law of the weight using the gradient descent method can be represented as:

$$\dot{v}_{kj}^{2} = -\eta_1 \frac{\partial R_1}{\partial v_{kj}^{2}} = -\eta_1 \frac{\partial R_1}{\partial y_k^{3}} \frac{\partial y_k^{3}}{\partial v_{kj}^{2}} = -\eta_1 \frac{\partial R_1}{\partial y_k^{3}} y_j^{2} \tag{35}$$

Comparing (33) with (35), yields $\partial R_1 / \partial y_k^3 = -eB_1$. The adaptation law of the recurrent weight v_{ik}^1 using the gradient descent method can be updated as:

$$\dot{v}_{ik}^{1} = -\eta_2 \frac{\partial R_1}{\partial v_{ik}^{1}} = \eta_2 B_1 \, e \, v_{kj}^{2} G_j^{\sigma}(\cdot) x_i^1(N) y_k^3(N-1) \tag{36}$$

where η_2 is the learning rate. In order to obtain a better convergence, the amended ABC optimization is proposed to adjust two better learning rates η_1 and η_2 of the weights in the modified recurrent Gegenbauer OPNN.

E. Amended ABC Optimization

The general algorithmic structure of ABC optimization [32-35] consists of an initialization phase, a worker bee phase, an onlooker bee phase and a scout bee phase. Firstly, two food sources (solutions), i.e. two learning rates, in the initialization phase are randomly initialized as follows:

$$\chi_{m,i} = \lambda_{i,\min} + \varphi_i(\lambda_{i,\max} - \lambda_{i,\min}), m = 1,2, \quad i = 1,2,\cdots,D \tag{37}$$

where $\chi_{m,i}$ is the value of the i dimension of the m solution. $\lambda_{i,\max}$ and $\lambda_{i,\min}$ represent the lower and upper bounds of the parameter $\chi_{m,i}$. φ_i is a random number within the range [0,1]. Then, the obtained solutions are evaluated and the objective function values of the clustering problem are calculated as $f_j(\chi_{m,i}) = \sum_{j=1}^{n_1} e_j / n_1$, where n_1 is the maximum cycle number (MCN). $f_j(\chi_{m,i})$ is the objective function value. e_j is the tracking error between the desired rotor speed ω_c and the actual rotor speed ω_r at j dimension of the m solution.

Secondly, the worker bee behavior in the worker bee phase is to find a better solution within the neighborhood of the solution ($\chi_{m,i}$). In the ABC optimization algorithm, this neighbor solution is determined as follows:

$$\begin{aligned} &\eta_{m,i} = \chi_{m,i} + \phi_{m,i}[\chi_{m,i} - \chi_{k,i}], \\ &m = 1,2, \quad i = 1,2,\cdots,D, \quad k = 1,2,\cdots,M \end{aligned} \tag{38}$$

where $\chi_{k,i}$ is a solution selected randomly. i is a randomly chosen dimension, and $\phi_{m,i}$ is a random number within the range [-1, 1]. After producing the new candidate solution $\eta_{m,i}$, its profitability is calculated. Then, a greed based selection is applied between $\eta_{m,i}$ and $\chi_{m,i}$. The fitness $fit(\chi_{m,i})$ of a solution can be calculated from its objective function value $f_j(\chi_{m,i})$ as follows:

$$fit(\chi_{m,i}) = \begin{cases} \dfrac{1}{1 + f_j(\chi_{m,i})}, & if \quad f_j(\chi_{m,i}) \geq 0 \\ 1 + \left| f_j(\chi_{m,i}) \right|, & if \quad f_j(\chi_{m,i}) < 0 \end{cases} \tag{39}$$

Thirdly, an onlooker in the onlooker bee phase chooses a food source to exploit depending on this information. In the ABC optimization algorithm, by using the fitness $fit(\chi_{m,i})$ of the solutions, the probability value z_m can be calculated as follows:

$$z_m = \frac{fit(\chi_{m,i})}{\sum_{m=1}^{N1} fit(\chi_{m,i})} \tag{40}$$

After a solution is selected, as in the worker bee phase, a neighbor solution is determined by using (38), and its fitness value is computed. Then, a greed based selection is applied between $\eta_{m,i}$ and $\chi_{m,i}$. Therefore, by attracting more onlookers to richer sources, positive feedback behavior appears. Finally, at the end of every cycle, trial counters of all of the solutions are controlled. If an abandonment is detected, the related worker bee is converted to a scout and takes a new randomly produced solution using (37). To balance the positive feedback in the scout bee phase, a negative feedback behavior arises. However, in the standard ABC optimization algorithm, this difference is not considered and artificial worker bees and onlookers determine a new candidate solution by using the same formula as (38). Meanwhile, the ABC optimization method possesses a slower convergence. Therefore, the amended ABC optimization algorithm [2] from (38) with an inertia weight is introduced for the behavior of onlookers. The amended ABC optimization algorithm [2] is given as follows:

$$\begin{aligned} &\eta_{m,i}^{a} = \mu_{m,i} \cdot \chi_{m,i}^{a} + \phi_{m,i}[\chi_{m,i}^{a} - \chi_{k,i}], \\ &m = 1,2, \quad i = 1,2,\cdots,D, \quad k = 1,2,\cdots,M \end{aligned} \tag{41}$$

$$\mu_{m,i} = \mu_{m,i-1} + \varphi_{m,i}(1 - \mu_{m,i-1}) \tag{42}$$

In this formula, $\eta_{m,i}^{a}$ represents the best solution among the neighbors of $\chi_{m,i}^{a}$ and itself with respect to two learning rates $\eta_m, m = 1, 2$. A similarity measure in terms of

the structure of the solutions can be used to determine a neighborhood for $\chi_{m,i}^{a}$. At this point, in order to define an appropriate neighborhood, different approaches can be used. In addition, for different representations of the solutions, different similarity measures can be defined. Hence, using the amended formula equations (41) and (42), a combinatorial problem can also be optimized using the amended ABC optimization algorithm [2]. For example, the neighborhood of a solution $\chi_{m,i}^{a}$ can be defined considering the mean Euclidean distance $E_{m,i}$ between $\chi_{m,i}^{a}$ and the rest of the solutions for the numerical optimization problems. The Euclidean distance $E_{m,i}$ between $\chi_{m,i}^{a}$ and $\chi_{k,i}$ can be calculated as:

$$E_{m,i} = [\sum_{i=1}^{i=D} (\chi_{m,i}^{a} - \chi_{k,i})^2]^{0.5}, i = 1,2,\cdots, D \qquad (43)$$

If there is a solution where the Euclidean distance from $\chi_{m,i}^{a}$ is less than the mean Euclidean distance $E_{Nm,i}$, it can be accepted as a neighbor of $\chi_{m,i}^{a}$. Based on the probability selection mechanism, if solutions are feasible, they are selected proportionally to their fitness values. Meanwhile, if solutions are infeasible, they are selected based on their constraint violation values. Onlooker bees produce modifications of the position of the selected solution using equations (41) and (42). The first and second terms in these equations are for improved exploration, and third term directs the search toward the best solution, which enhances the exploitation ability. Then the best solution, which is memorized, can be achieved.

IV. Experimental Results

The whole structure of the six-phase CRIM driving CVT system by means of a TMS320F28335 DSP control system and a mixed signal FPGA system is shown in Fig. 2. A photo of the experimental setup is shown in Fig. 5. The proposed control algorithm was executed using the TMS320F28335 DSP control system including 16 channel 12-bit analog-to-digital (A/D) converters, 18 programmable PWM ports, 6 channel high-resolution PWM ports and 2 quadrature encoder interfaces.

A flowchart of the executed control methodologies with real-time implementation by means of a DSP control system and a mixed signal FPGA system is comprised of the main program and the interrupt service routine (ISR) as shown in Fig. 6. In the main program, the parameters and input/output (I/O) initialization are processed first. Then, the interrupt interval for the ISR is set. After enabling the interrupt, the main program is used to monitor the control data. An ISR with a 2 *ms* sampling interval is used for reading the rotor position of the six-phase CRIM driving CVT system from

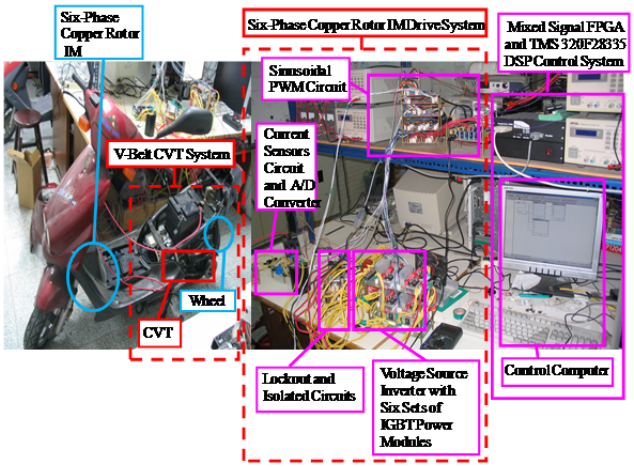

Fig. 5. A photo of the experimental setup.

the encoder and for reading the six-phase current from the A/D converters. It is also used for calculating the rotor position and speed, executing the lookup table and coordinate translation, executing the PI current control, executing the proposed control system, and outputting the six-phase sinusoidal PWM signal to switch the six sets of IGBT power modules voltage source inverter with a switching frequency of 15 *k*Hz via the interlock and isolated circuits.

The two identifiers si_d and si_dmax, shown in Fig. 6, are provided to execute the indirect field-oriented control by the mixed signal FPGA system. The identifier si_a is provided to execute the proposed control scheme by the TMS320F28335 DSP control system. The two initial values si_d and si_a are set to zero. The initial value si_dmax is set to five. When the indirect field-oriented control executed by the mixed signal FPGA system is implemented less than five times, i.e., si_d<si_dmax, the indirect field-oriented control must be continuously executed by the mixed signal FPGA system. When the proposed control scheme executed by the TMS320F28335 DSP control system is implemented one time, the identifier si_a is set to 1, i.e., si_a=1. Then the procedure returns to the original starting point. Therefore, the indirect field-oriented control executed by the mixed signal FPGA system is implements five times, then the proposed control scheme executed by the TMS320F28335 DSP control system is implemented one time. This procedure is implemented online by the TMS320F28335 DSP control system and the mixed signal FPGA system.

The specification of the six-phase CRIM are: six-phase 48 V, 1.5 kW, and 3458 *rpm*. The parameters of the six-phase CRIM are given as follows: $k_a = 0.86\ Nm/A$, $\bar{J}_{1a} = 45.15\times10^{-3}\ Nms$, $\bar{B}_{1a} = 2.12\times10^{-3}\ Nms/rad$, $L_{ss} = 4.52\ mH$, $L_{rr} = 4.32\ mH$, $L_M = 2.64\ mH$, $r_s = 2.2\Omega$, and $r'_r = 1.8\Omega$. Owing to the inherent uncertainty in the CVT system (e.g. the lumped nonlinear external disturbances and parameter variations) and the output current limitation of the battery capacity, the six-phase

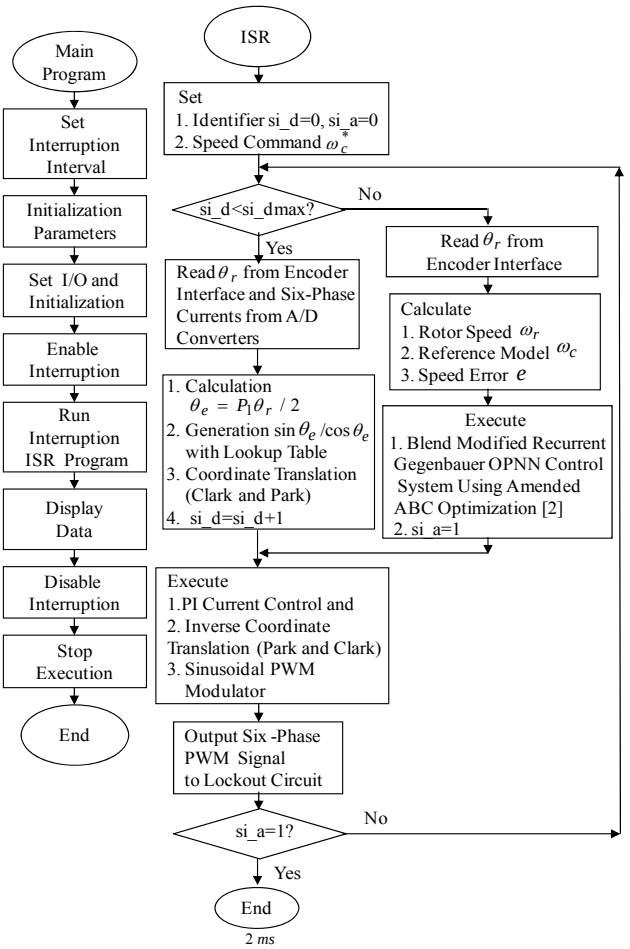

Fig. 6. Flowchart of the executing program by using DSP control system and mixed signal FPGA system.

CRIM can only operate at 314 *rad/s* (3000 *rpm*) to avoid burning the IGBT module of the CVT system at high speed perturbations.

Two experimentation tests are provided to compare the control performances of the PI controller, the three-layer feedforward NN control system and the blend modified recurrent Gegenbauer OPNN control system using an amended ABC optimization [2]. One is the 157 *rad/s* (1500 *rpm*) case under lumped nonlinear external disturbances with parameter variations $T_1^l = \Delta T_1 + T_{u1}$, and the other is the 314 *rad/s* (3000 *rpm*) case under lumped nonlinear external disturbances with two times the parameter variations $T_1^l = 2\Delta T_1 + T_{u1}$.

Firstly, all of the gains of the well-known PI controller through some heuristic knowledge [46-48] on the tuning of PI controllers are $k_{ps} = 15.1$ and $k_{is} = k_{ps} / T_{is} = 3.2$ in the 157 *rad/s* (1500 *rpm*) case under lumped nonlinear external disturbances with parameter variations $T_1^l = \Delta T_1 + T_{u1}$ for the speed tracking to achieve good transient and steady-state control performance. Secondly, the three-layer feedforward NN control system has two, three, and one neurons in the input, the hidden, and the output layers, respectively. It adopts the sigmoid activation function in the input layer and the hidden layer. Moreover, the connective weight between the input layer and the hidden layer, and the connective weight between the hidden layer and the output layer in the three-layer feedforward NN are initialized with random numbers. All of the learning rates of the two kinds of connective weights are chosen as fixed constants. The parameter adjustment process remains continually active for the duration of the experimentation. The gains of the three-layer feedforward NN control system are chosen to achieve the best transient control performance while considering the requirement of stability. Thirdly, the control gains of the blend modified recurrent Gegenbauer OPNN control system using an amended ABC optimization [2] are $\delta = 0.5$, $\beta = 0.1$. All of the control gains of the blend modified recurrent Gegenbauer OPNN control system using an amended ABC optimization [2] are chosen to achieve the best transient control performance while considering the requirement of stability. The parameter adjustment process remains continually active for the duration of the experiment. The structure of the modified recurrent Gegenbauer OPNN controller has two nodes, three nodes, and one node in the input layer, the hidden layer, and the output layer, respectively.

The tracking responses of the command rotor speed ω_c^*, the desired command rotor speed ω_c, and the measured rotor speed ω_1 using the well-known PI controller, the three-layer feedforward NN control system and the blend modified recurrent Gegenbauer OPNN control system with an amended ABC optimization [2] for the six-phase CRIM driving CVT system at 157 *rad/s* (1500 *rpm*) under lumped nonlinear external disturbances and with parameter variations $T_1^l = \Delta T_1 + T_{u1}$ are shown in Figs. 7(a), 7(b) and 7(c), respectively. The tracking responses of the speed error e while using the well-known PI controller, the three-layer feedforward NN control system and the blend modified recurrent Gegenbauer OPNN control system with an amended ABC optimization [2] for the six-phase CRIM driving CVT system at 157 *rad/s* (1500 *rpm*) under lumped nonlinear external disturbances and with parameter variations $T_1^l = \Delta T_1 + T_{u1}$ are shown in Figs. 8(a), 8(b) and 8(c), respectively.

The maximum errors of e while using the well-known PI controller, the three-layer feedforward NN control system and the blend modified recurrent Gegenbauer OPNN control system with an amended ABC optimization [2] at 157 *rad/s* (1500 *rpm*) under lumped nonlinear external disturbances and with parameter variations $T_1^l = \Delta T_1 + T_{u1}$ are 9.5 *rad/s* (91 *rpm*), 7.5 *rad/s* (72 *rpm*) and 4.5 *rad/s* (43 *rpm*), respectively;

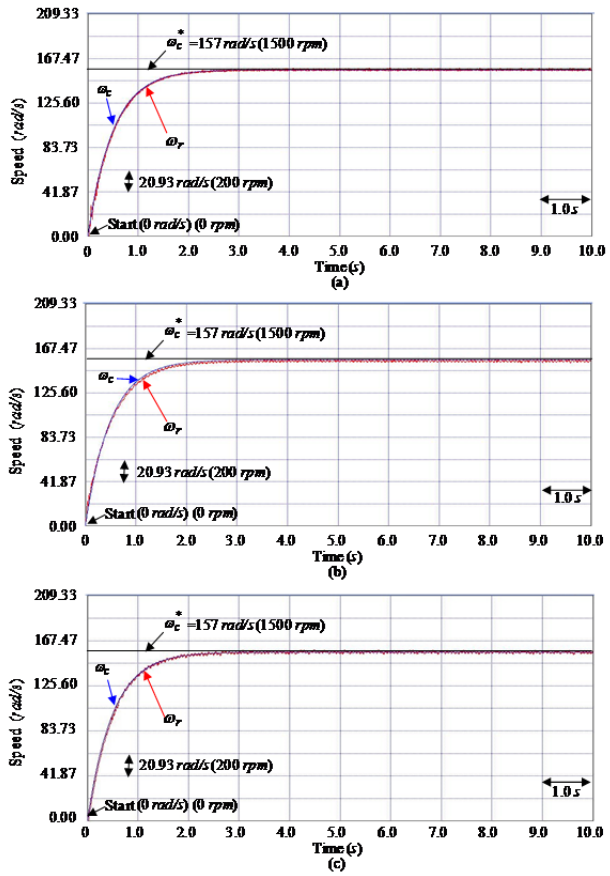

Fig. 7. Experimental results of tracking response of the command rotor speed ω_c^*, desired command rotor speed ω_c, and measured rotor speed ω_r for the six-phase CRIM driving CVT system at 157 *rad/s* (1500 *rpm*) case under lumped nonlinear external disturbances and with parameter variations $T_1^l = \Delta T_1 + T_{u1}$. (a) Using the well-known PI controller. (b) Using the three-layer feedforward NN control system. (c) Using the blend modified recurrent Gegenbauer OPNN control system with an amended ABC optimization [2].

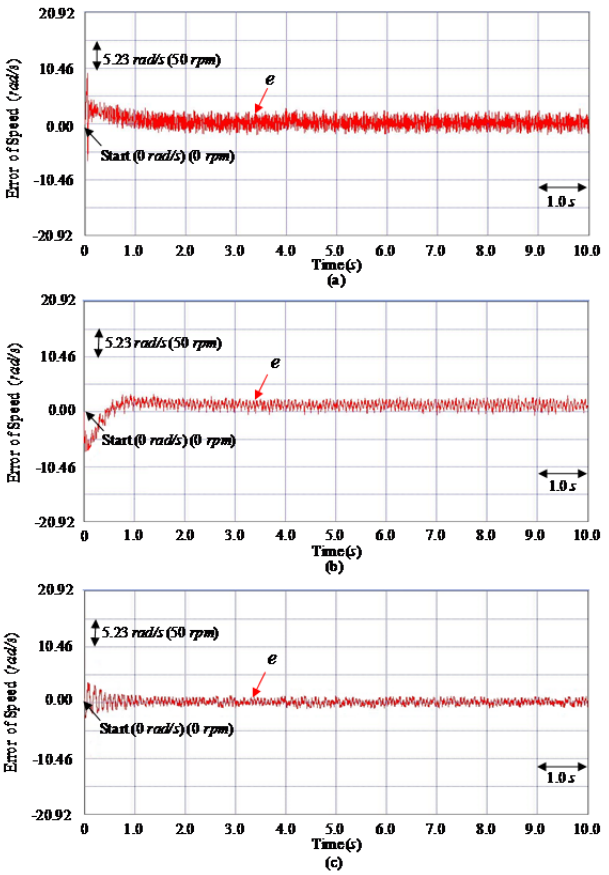

Fig. 8. Experimental results of tracking responses of the speed error e for the six-phase CRIM driving CVT system at 157 *rad/s* (1500 *rpm*) case under lumped nonlinear external disturbances and with parameter variations $T_1^l = \Delta T_1 + T_{u1}$. (a) Using the well-known PI controller. (b) Using the three-layer feedforward NN control system. (c) Using the blend modified recurrent Gegenbauer OPNN control system with an amended ABC optimization [2].

and RMS errors of e are 5.0 *rad/s* (48 *rpm*), 3.5 *rad/s* (33 *rpm*) and 2.0 *rad/s* (19 *rpm*), respectively.

The responses of the command electromagnetic torque T_1 while using the well-known PI controller, the three-layer feedforward NN control system and the blend modified recurrent Gegenbauer OPNN control system using an amended ABC optimization [2] for the six-phase CRIM driving CVT system at 157 *rad/s* (1500 *rpm*) under lumped nonlinear external disturbances and with parameter variations $T_1^l = \Delta T_1 + T_{u1}$ are shown in Figures 9(a), 9(b) and 9(c), respectively. Because low speed operation is the same as the nominal case which is $T_1 \cong T_1^l$ operation because of smaller disturbances, the tracking responses of the speed and current while using the well-known PI controller, the three-layer feedforward NN control system and the blend modified recurrent Gegenbauer OPNN control system with an amended ABC optimization [2] for the six-phase CRIM driving CVT system has better tracking performance.

In addition, the tracking responses of the command rotor speed ω_c^*, the desired command rotor speed ω_c, and the measured rotor speed ω_r while using the well-known PI controller, the three-layer feedforward NN control system and the blend modified recurrent Gegenbauer OPNN control system with an amended ABC optimization [2] for the six-phase copper rotor IM servo-drive CVT system at 314 *rad/s* (3000 *rpm*) under lumped nonlinear external disturbances and with two times the parameter variations $T_1^l = 2\Delta T_1 + T_{u1}$ are shown in Figs. 10(a), 10(b) and 10(c), respectively.

The tracking responses of the speed error e while using the well-known PI controller, the three-layer feedforward NN control system and the blend modified recurrent Gegenbauer OPNN control system with an amended ABC optimization [2] for the six-phase copper rotor IM driving CVT system at

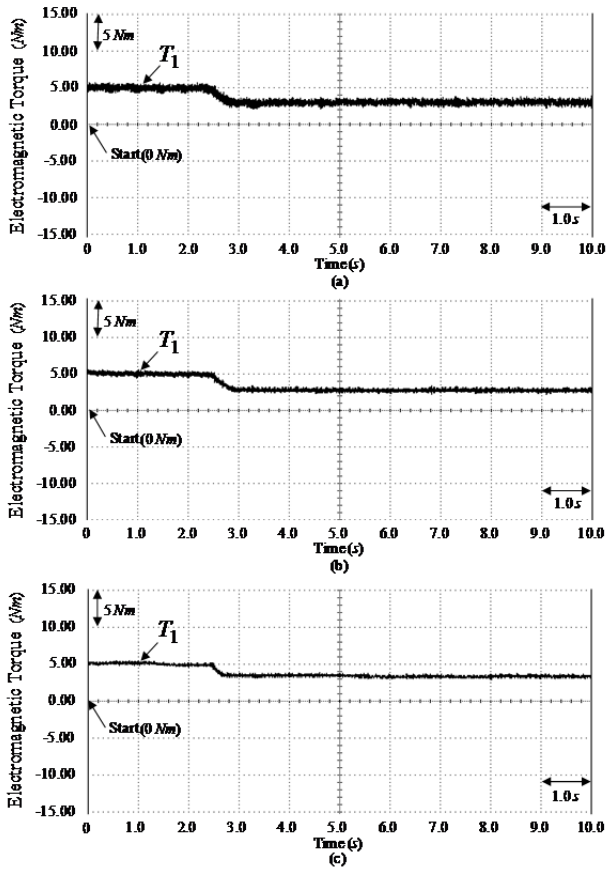

Fig. 9. Experimental results of responses of the command electromagnetic torque T_1 for the six-phase CRIM driving CVT system at 157 *rad/s* (1500 *rpm*) case under lumped nonlinear external disturbances and with parameter variations $T_1^l = \Delta T_1 + T_{u1}$. (a) Using the well-known PI controller. (b) Using the three-layer feedforward NN control system. (c) Using the blend modified recurrent Gegenbauer OPNN control system with an amended ABC optimization [2].

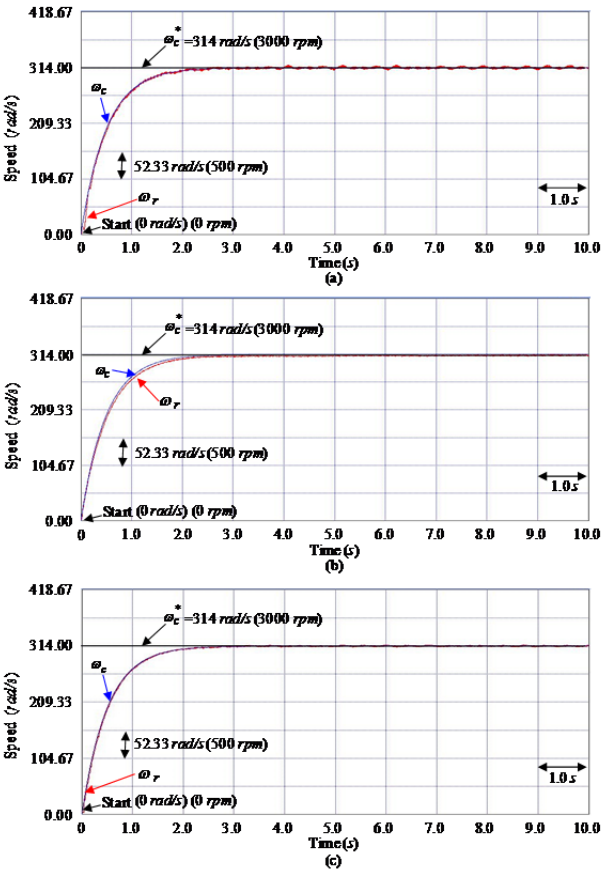

Fig. 10. Experimental results of tracking response of the command rotor speed ω_c^*, desired command rotor speed ω_c, and measured rotor speed ω_r for the six-phase CRIM driving CVT system at 314 *rad/s* (3000 *rpm*) case under lumped nonlinear external disturbances and with two times the parameter variations $T_1^l = 2\Delta T_1 + T_{u1}$. (a) Using the well-known PI controller. (b) Using the three-layer feedforward NN control system. (c) Using the blend modified recurrent Gegenbauer OPNN control system with an amended ABC optimization [2].

314 *rad/s* (3000 *rpm*) under lumped nonlinear external disturbances and with two times the parameter variations $T_1^l = 2\Delta T_1 + T_{u1}$ are shown in Figs. 11(a), 11(b) and 11(c), respectively. The tracking response of the speed shown in Figs. 10(a) leads to degenerate tracking in the presence of larger nonlinear disturbances (e.g. rolling resistance, wind resistance, and parameter variation) under high speed operation. A sluggish tracking response of the speed is obtained for the six-phase CRIM driving CVT system using the well-known PI controller. The linear controller has weak robustness under larger nonlinear disturbances due to the lack of appropriately gains tuning or the lack of a degenerate nonlinear effect.

The maximum errors of e while using the well-known PI controller, the three-layer feedforward NN control system and the blend modified recurrent Gegenbauer OPNN control system with an amended ABC optimization [2] at 314 *rad/s* (3000 *rpm*) under lumped nonlinear external disturbances and with two times the parameter variations $T_1^l = 2\Delta T_1 + T_{u1}$ are 22.8 *rad/s* (218 *rpm*), 9.5 *rad/s* (91 *rpm*) and 5.2 *rad/s* (50 *rpm*), respectively; and RMS errors of e are 6.5 *rad/s* (62 *rpm*), 3.5 *rad/s* (33 *rpm*) and 2.5 *rad/s* (24 *rpm*), respectively.

The responses of the command electromagnetic torque T_1 while using the well-known PI controller, the three-layer feedforward NN control system and the blend modified recurrent Gegenbauer OPNN control system with an amended ABC optimization [2] for the six-phase CRIM driving CVT system at 314 *rad/s* (3000 *rpm*) under lumped nonlinear external disturbances and with two times the parameter variations $T_1^l = 2\Delta T_1 + T_{u1}$ are shown in Figs. 12(a), 12(b) and 12(c), respectively. Additionally, the dynamic response of the command electromagnetic torque shown in Fig. 12(b) while using three-layer feedforward NN control system generates a high torque ripple in the CVT

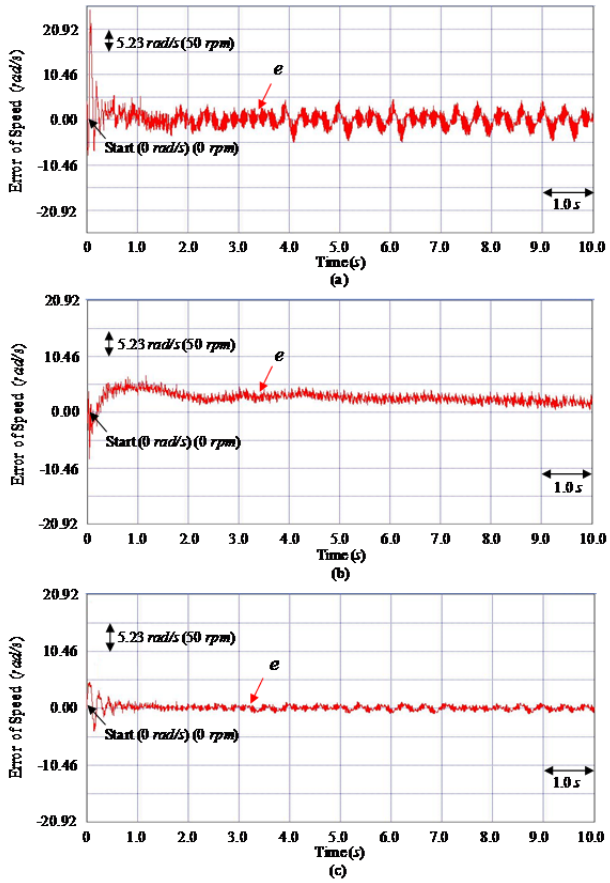

Fig. 11. Experimental results of tracking responses of the speed error e for the six-phase CRIM driving CVT system at 314 *rad/s* (3000 *rpm*) case under lumped nonlinear external disturbances and with two times the parameter variations $T_1^l = 2\Delta T_1 + T_{u1}$. (a) Using the well-known PI controller. (b) Using the three-layer feedforward NN control system. (c) Using the blend modified recurrent Gegenbauer OPNN control system with an amended ABC optimization [2].

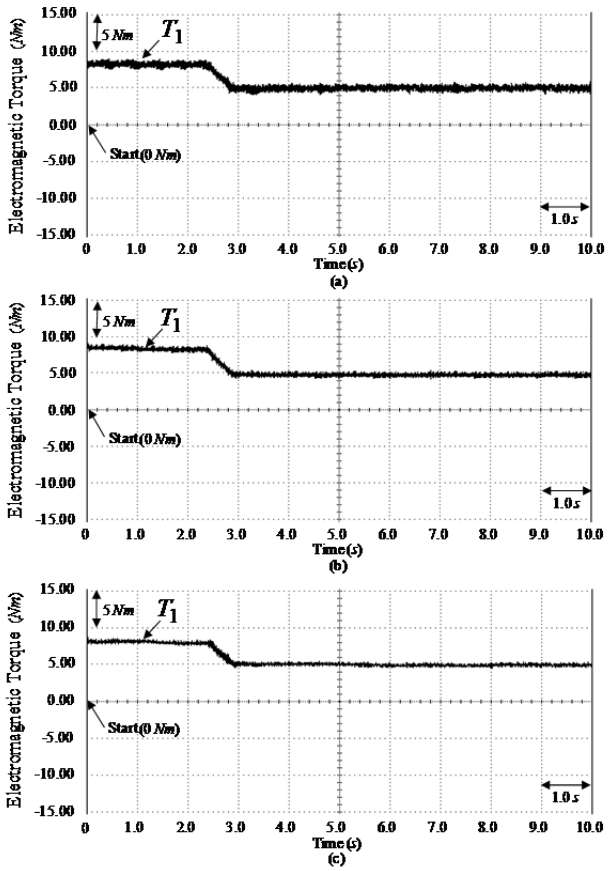

Fig. 12. Experimental results of responses of the command electromagnetic torque T_1 for the six-phase CRIM driving CVT system at 314 *rad/s* (3000 *rpm*) case under lumped nonlinear external disturbances and with two times the parameter variations $T_1^l = 2\Delta T_1 + T_{u1}$. (a) Using the well-known PI controller. (b) Using the three-layer feedforward NN control system. (c) Using the blend modified recurrent Gegenbauer OPNN control system with an amended ABC optimization [2].

system under nonlinear disturbances such as V-belt shaking friction and action friction between the primary pulley and the secondary pulley. Meanwhile, the electromagnetic torque T_1 while using the blend modified recurrent Gegenbauer OPNN control system with an amended ABC optimization [2] generates a lower torque ripple, as shown in Fig. 12(c).

The tracking response of the speed while using the blend modified recurrent Gegenbauer OPNN control system and an amended ABC optimization [2] are shown in Figs. 7(c) and 10(c) under larger lumped nonlinear external disturbances and parameter variations. Accurate tracking performance was achieved for the six-phase CRIM driving CVT system when the blend modified recurrent Gegenbauer OPNN control system with an amended ABC optimization [2] was used, because of the online adaptive mechanism of the modified recurrent Gegenbauer OPNN and the operation of the recompensed controller. The dynamic response of the command electromagnetic torque T_1 shown in Fig. 12(c) brings about a lower torque ripple due to the online adjustment of the modified recurrent Gegenbauer OPNN to cope with the high-frequency unmodelled dynamic of the CVT system's nonlinear disturbances, such as V-belt shaking friction and action friction between the primary pulley and the secondary pulley. Therefore, these experimental results show that the blend modified recurrent Gegenbauer OPNN control system with an amended ABC optimization [2] has better control performance than the well-known PI controller and the three-layer feedforward NN control system at high speed perturbations and lumped nonlinear external disturbances for the six-phase CRIM driving CVT system.

In addition, the convergence responses of the two varied learning rates η_1 and η_2 of the modified recurrent Gegenbauer orthogonal polynomial NN using an amended ABC optimization [2] at 157 *rad/s* (1500 *rpm*) under lumped nonlinear external disturbances and with parameter variations $T_1^l = \Delta T_1 + T_{u1}$; and at 314 *rad/s* (3000 *rpm*) under lumped nonlinear external disturbances and with two times the

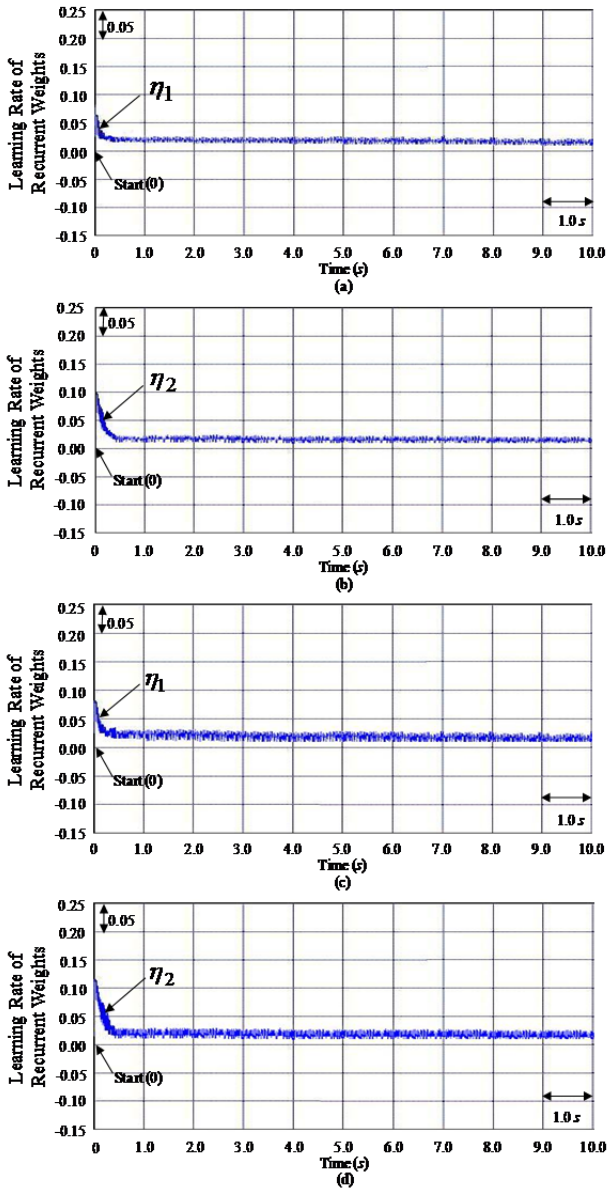

Fig. 13. Experimental results of convergence responses for the modified recurrent Gegenbauer OPNN control system using an amended ABC optimization [2]: (a) learning rates η_1 at 157 *rad/s* (1500 *rpm*) under lumped nonlinear external disturbances and with parameter variations $T_1^l = \Delta T_1 + T_{u1}$. (b) Learning rates η_2 at 157 *rad/s* (1500 *rpm*) under lumped nonlinear external disturbances and with parameter variations $T_1^l = \Delta T_1 + T_{u1}$. (c) Learning rates η_1 at 314 *rad/s* (3000 *rpm*) under lumped nonlinear external disturbances and with two times the parameter variations $T_1^l = 2\Delta T_1 + T_{u1}$. (d) Learning rates η_2 at 314 *rad/s* (3000 *rpm*) under lumped nonlinear external disturbances and with two times the parameter variations $T_1^l = 2\Delta T_1 + T_{u1}$.

parameter variations $T_1^l = 2\Delta T_1 + T_{u1}$ are shown in Figs. 13(a), 13(b) and Figs. 13(c), 13(d), respectively. The convergence responses of the two varied learning rates η_1

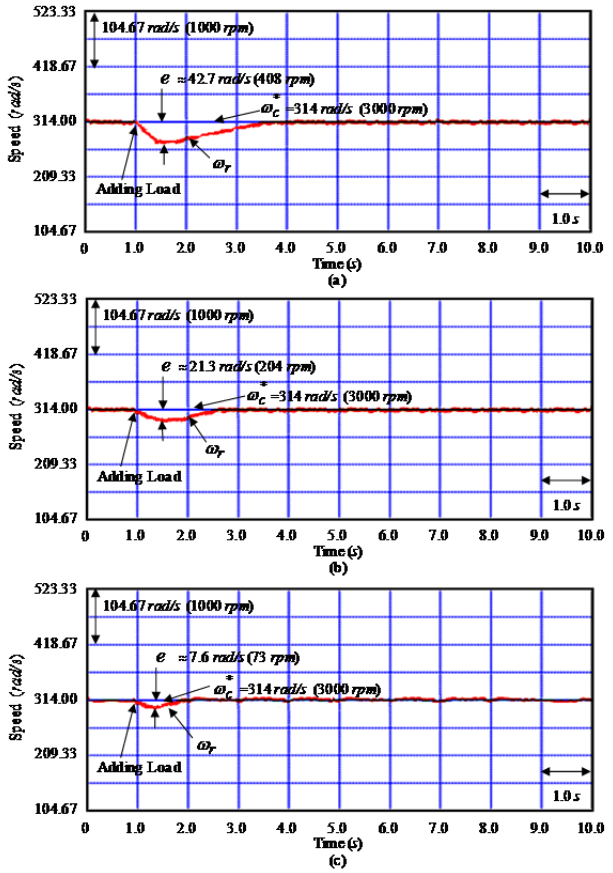

Fig. 14. Experimental results of speed-adjusted response of the command rotor speed ω_c^* and the measured rotor speed ω_r under $T_1^l = 2Nm\,(T_{a1}) + T_{u1}$ load disturbances with adding load at 314 *rad/s* (3000 *rpm*). (a) Using the well-known PI controller. (b) Using the three-layer feedforward NN control system. (c) Using the blend modified recurrent Gegenbauer OPNN control system with an amended ABC optimization [2].

and η_2 of the modified recurrent Gegenbauer OPNN using an amended ABC optimization [2] have faster convergence speed than the two fixed learning rates of the modified recurrent Gegenbauer OPNN. From the above results, it can be easily observed that the proposed amended ABC optimization can provide a more accurate optimal solution and converges to the criteria with a higher probability than the conventional ABC optimization.

Finally, the conditions under load torque disturbances and parameter variations $T_1^l = 2\,Nm\,(T_{a1}) + T_{u1}$ while adding a load at measured rotor speed responses are tested. The measured rotor speed response of the load regulation when the well-known PI controller, the three-layer feedforward NN control system, and the blend modified recurrent Gegenbauer OPNN control system with an amended ABC optimization [2] were used under load torque disturbances and parameter variations $T_1^l = 2Nm(T_{a1}) + T_{u1}$ while adding a load at 314 *rad/s* (3000 *rpm*) are shown in Figs. 14(a), 14(b) and 14(c),

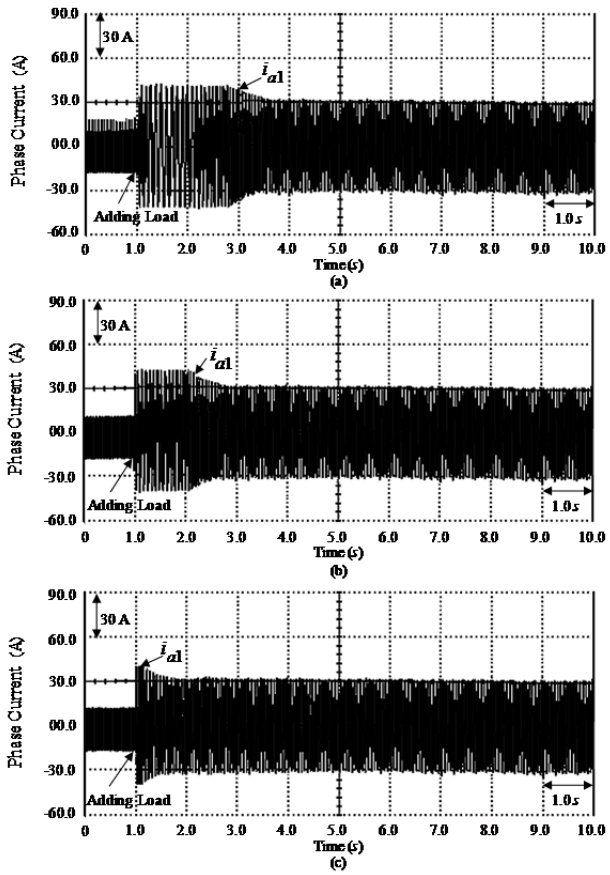

Fig. 15. Experimental results of response of the measured current i_{a1} in phase *a1* under $T_l^l = 2Nm(T_{a1}) + T_{u1}$ load disturbances with adding load at 314 *rad/s* (3000 *rpm*). (a) Using the well-known PI controller. (b) Using the three-layer feedforward NN control system. (c) Using the blend modified recurrent Gegenbauer OPNN control system with an amended ABC optimization [2].

respectively.

Experimental results of the measured current in phase *a*1 when the well-known PI controller, the three-layer feedforward NN control system, and the blend modified recurrent Gegenbauer OPNN control system with an amended ABC optimization [2] were used under load torque disturbances and parameter variations $T_l^l = 2Nm(T_{a1}) + T_{u1}$ when adding a load at 314 *rad/s* (3000 *rpm*) are shown in Figs. 15(a), 15(b) and 15(c), respectively. These experimental results show that the degenerated responses under load torque disturbances and parameter variations $T_l^l = 2Nm(T_{a1}) + T_{u1}$ while adding a load are considerably improved when the blend modified recurrent Gegenbauer OPNN control system with an amended ABC optimization [2] is used. Moreover, the transient response of the blend modified recurrent Gegenbauer OPNN control system with an amended ABC optimization [2] shows a faster convergence and a more favorable load regulation than that of the well-known PI controller and the three-layer feedforward NN control system.

TABLE I
PERFORMANCE COMPARISONS OF CONTROL SYSTEMS

Control System / Characteristic Performance	Well-Known PI Controller	Three-layer Feedforward NN Control System	Blend Modified Recurrent Gegenbauer OPNN Control System with an Amended ABC Optimization [2]
Dynamic Response	Slow	Fast	Faster
Load Regulation Capability	Poor	Good	Best
Convergence Speed	Low	Middle	High
Torque Ripple (V-belt Shaking Friction, Action Friction between the Primary Pulley and the Secondary Pulley)	High (5% of (maximum torque-minimum torque)/average torque)	Middle (2.5% of (maximum torque-minimum torque)/average torque)	Low (1% of (maximum torque-minimum torque)/average torque)

In addition, a characteristic performance comparison between the well-known PI controller, the three-layer feedforward NN control system and the blend modified recurrent Gegenbauer OPNN control system with an amended ABC optimization [2] is presented in Table 1 on the basis of experimental results. The values of the dynamic response while using the well-known PI controller, the three-layer feedforward NN control system and the blend modified recurrent Gegenbauer OPNN control system with an amended ABC optimization [2] at 314 *rad/s* (3000 *rpm*) under lumped nonlinear external disturbances and with two times the parameter variations $T_l^l = 2\Delta T_l + T_{u1}$ are 0.5 *s*, 0.25 *s* and 0.1 *s*, respectively. The values of the torque ripple while using the well-known PI controller, the three-layer feedforward NN control system and the proposed blend modified recurrent Gegenbauer OPNN control system with an amended ABC optimization [2] at 314 *rad/s* (3000 *rpm*) under lumped nonlinear external disturbances and with two times the parameter variations $T_l^l = 2\Delta T_l + T_{u1}$ are 5%, 2.5% and 1% of the (maximum torque-minimum torque)/average torque, respectively. In Table I, the various performances of the blend modified recurrent Gegenbauer OPNN control system with an amended ABC optimization [2] is superior to those of the well-known PI controller and the three-layer feedforward NN control system.

V. CONCLUSIONS

A blend modified recurrent Gegenbauer OPNN control system using an amended ABC optimization [2] with robust control characteristics has been successfully developed for the purpose of controling six-phase CRIM driving CVT

systems. The blend modified recurrent Gegenbauer OPNN control system with an amended ABC optimization [2] can perform overseer control based on the uncertainty bounds of the controlled system on the basis of the uncertainty bounds of the controlled system. In addition, it was designed to stabilize the system states within a predetermined bound area. The blend modified recurrent Gegenbauer OPNN control system with an amended ABC optimization [2], which can perform overseer control, modified recurrent Laguerre OPNN control and recompensed control, was proposed to reduce and smooth the control effort when the system states are within a predetermined bound area.

The main contributions of this study are as follows: 1. simplified dynamic models of a CVT system driven by a six-phase CRIM with unknown nonlinear and time-varying characteristics were successfully derived, 2. the blend modified recurrent Gegenbauer OPNN control system with an amended ABC optimization [2] for a six-phase CRIM driving CVT system under the occurrence of lumped nonlinear load disturbances was successfully applied to enhance robustness, 3. the adaptation law of online parameters tuning in the modified recurrent Gegenbauer OPNN and the estimation law of the reimbursed controller were successfully derived using the Lyapunov stability theorem, 4. an amended ABC optimization was used to successfully apply two varied learning rates for the connective weights and recurrent weights in the modified recurrent Gegenbauer OPNN for achieving faster convergence, 5. the blend modified recurrent Gegenbauer OPNN control system with an amended ABC optimization [2], has an improved online learning capability for quickly capturing the nonlinear and time-varying behavior of a system, and 6. the blend modified recurrent Gegenbauer OPNN control system with an amended ABC optimization [2] has a lower torque ripple than the well-known PI controller and the three-layer feedforward NN control.

Finally, the control performance of the blend modified recurrent Gegenbauer OPNN control system using an amended ABC optimization [2] is better suited to six-phase CRIM driving CVT systems when compared with the well-known PI controller and the three-layer feedforward NN control.

ACKNOWLEDGMENT

The author would like to acknowledge the financial support of the Ministry of Science and Technology of Taiwan under grant MOST 104-2221-E-239 -011.

REFERENCES

[1] K. K. Mahopatra, K. Gopalkumar, V.T. Somasekhar L. Umanand, "A novel scheme for six phase induction motor with open end windings," *28th Annual Conference of IEEE Industrial Electronics Society*, Spain, 5-8 Nov. 2002, pp. 810-815.

[2] C. H. Lin. "Modelling and control of six-phase induction motor servo-driven continuously variable transmission system using blend modified recurrent Gegenbauer orthogonal polynomial neural network control system and amended artificial bee colony optimization," *International Journal of Numerical Modelling Electronic Networks Devices and Fields*, DOI: 10.1002/jnm.2154, Record online: 17 Mar. 2016.

[3] E. F. Brush, J. L. Kirtley, and D. T. Peters, "Die-cast copper rotors as strategy for improving induction motor efficiency," *Electrical Insulation Conference and Electrical Manufacturing Expo.*, Nashville, Tennessee, USA, 2007, pp. 322-327.

[4] D. Liang, X. Yang, J. Yu, and V. Zhou, "Experience in China on the die-casting of copper rotors for induction motors," *IEEE Intl. Conference on Electrical Machines*, Marseille, France, 2012, pp. 254-258.

[5] A. R. Munoz and T. A. Lipo, "Dual stator winding induction machine drive," *IEEE Trans. Ind. Appl.*, Vol. 36, No. 5, pp. 1369-1379, Sep./Oct. 2000.

[6] R. Bojoi, M. Lazzari, F. Profumo, and A. Tenconi, "Digital field-oriented control for dual three-phase induction motor drives," *IEEE Trans. Ind. Appl.*, Vol. 39, No. 3, pp. 752-760, May/Jun. 2013.

[7] G. K. Singh, K. Nam, and S. K. Lim, "A simple indirect field-oriented control scheme for multiphase induction machine," *IEEE Trans. Ind. Electron.*, Vol. 52, No.12, pp. 1177-1184, Aug. 2005.

[8] O. Ojo and I. E. Davidson, "PWM-VSI inverter assisted stand-alone dual stator winding induction generator," *IEEE Trans. Industry Applications*, Vol. 36, No. 6, pp. 1604-1611, Nov./Dec. 2000.

[9] C. Y. Tseng, L. W. Chen, Y. T. Lin, and J. Y. Li, "A hybrid dynamic simulation model for urban scooters with a mechanical-type CVT," *IEEE Intl. Conference on Automation and Logistics*, Qingdao, China, 2008, pp. 519-519.

[10] C. Y. Tseng, Y. F. Lue, Y. T. Lin, J. C. Siao, C. H. Tsai, and L. M. Fu, "Dynamic simulation model for hybrid electric scooters," *IEEE Intl. Symposium on Industrial Electronics*, Seoul, Korea, 2009, pp. 1464-1469.

[11] L. Guzzella, and A. M. Schmid, "Feedback linearization of spark-ignition engines with continuously variable transmissions," *IEEE Trans. Control Systems Technology*, Vol. 3, No.1, pp. 54-58, Mar. 1995.

[12] W. Kim and G. Vachtsevanos, "Fuzzy logic ratio control for a CVT hydraulic module," *Proceedings of the IEEE Symposium on Intelligent Control,* Rio, Greece, 2000, pp 151-156.

[13] G. Carbone, L. Mangialardi, B. Bonsen, C. Tursi, and P. A. Veenhuizen, "CVT dynamics: Theory and experiments," *Mechanism and Machine Theory*, Vol. 42, No. 4, pp. 409-428, Apr. 2007.

[14] N. Srivastava and I. Haque, "Transient dynamics of metal V-belt CVT: Effects of bandpack slip and friction characteristic," *Mechanism and Machine Theory*, Vol. 43, No. 4, pp. 457-479, Apr. 2008.

[15] N. Srivastava and I. Haque, "A review on belt and chain continuously variable transmissions (CVT): dynamics and control," *Mechanism and Machine Theory,* Vol. 44, No. 1, pp. 19-41, Jan. 2009.

[16] C. H. Lin, 'Composite recurrent Laguerre orthogonal polynomials neural network dynamic control for

continuously variable transmission system using altered particle swarm optimization," *Nonlinear Dynamics,* Vol. 81, pp. 1219-1245, Aug. 2015.
[17] K. S. Narendra and K. Parthasarathy, "Identification and control of dynamical system using neural networks," *IEEE Trans. Neural Networks*, Vol. 1, No. 1, pp. 4-27, Mar. 1990.
[18] P. S. Sastry, G. Santharam and K. P. Unnikrishnan, "Memory neural networks for identification and control of dynamical systems," *IEEE Trans. Neural Networks*, Vol. 5, No. 3, pp. 306-319, Mar. 1994.
[19] M. N. Eskander, "Minimization of losses in permanent magnet synchronous motors using neural network," *Journal of Power Electronics,* Vol. 2, No. 3, pp 220-229, Jul. 2002.
[20] A. F. Payam, M. N. Hashemnia and J. Faiz, "Robust DTC control of doubly-fed induction machines based on input-output feedback linearization using recurrent neural networks," *Journal of Power Electronics,* Vol. 11, No. 5, pp. 719-725, Sep. 2011.
[21] C. H. Lin, "Novel adaptive recurrent Legendre neural network control for PMSM servo-drive electric scooter," *J. Dynamic Systems, Measurement, and Control-Transactions of the ASME*, Vol. 137, No. 1, 12 pages, Jan. 2015.
[22] C. H. Lin, "A backstepping control of LSM drive systems using adaptive modified recurrent Laguerre OPNNUO," *Journal of Power Electronics*, Vol. 16, No. 2, pp. 598-609, Mar. 2016.
[23] C. H. Lin, "Design of a composite recurrent Laguerre orthogonal polynomial neural network control system with ameliorated particle swarm optimization for a continuously variable transmission system," *Control Engineering Practice*, Vol. 49, pp. 42-59, Apr. 2016.
[24] S. Belmehdi, "Generalized Gegenbauer orthogonal polynomials," *Intl. J. Computational and Applied Mathematic*s, Vol. 133, No. 1-2, pp. 195-205, Aug. 2001.
[25] C. Wu, H. Zhang, and T. Fang, "Flutter analysis of an airfoil with bounded random parameters in incompressible flow via Gegenbauer polynomial approximation," *Aerospace Science and Technology*, Vol. 11, No. 7-8, pp. 518-526, Nov./Dec.2007.
[26] Y. Zhang and W. Li, "Gegenbauer neural network and its weights-direct determination method," *IET Electronics Letters*, Vol. 45, No. 23, pp. 1184-1185, Nov. 2009.
[27] T. W. S. Chow and Y. Fang, "A recurrent neural-network-based real-time learning control strategy applying to nonlinear systems with unknown dynamics," *IEEE Trans. Ind. Electron.*, Vol. 45, No.1, pp. 151-161, Feb. 1998.
[28] X. D. Li, J. K. L. Ho, and T. W. S. Chow, "Approximation of dynamical time-variant systems by continuous-time recurrent neural networks," *IEEE Trans. Circuits Syst. II, Exp. Briefs*, Vol. 52, No. 10, pp. 656-660, Oct. 2005.
[29] C. H. Lin, "Recurrent modified Elman neural network control of PM synchronous generator system using wind turbine emulator of PM synchronous servo motor drive," *Intl. J. Electrical Power and Energy Systems,* Vol. 52, pp. 143-160, Nov. 2013.
[30] C. H. Lin, "Dynamic control for permanent magnet synchronous generator system using novel modified recurrent wavelet neural network," *Nonlinear Dynamics* Vol. 77, No. 4, pp. 1261-1284, Sep. 2014.
[31] C. H. Lin, "PMSM servo drive for V-belt continuously variable transmission system using hybrid recurrent Chebyshev NN control system," *J. Electrical Engineering and Technology*, Vol. 10, No.1, pp. 408-421, Feb. 2015.
[32] D. Karaboga, *An Idea Based on Honey Bee Swarm for Numerical Optimization,* Technical Report TR06, Computer Engineering Department, Erciyes University, Turkey, 2005.
[33] D. Karaboga and B. Basturk, "A powerful and efficient algorithm for numerical function optimization: artificial bee colony (ABC) algorithm," *J. Global Optimization*, Vol. 39, No. 3, pp. 459-471, Nov. 2007.
[34] D. Karaboga and B. Basturk, "Artificial bee colony (ABC) optimization algorithm for solving constrained optimization problems," *Lecture Notes in Artificial Intelligence*, Vol. 4529, pp. 789-798, Jun. 2007.
[35] D. Karaboga and B. Basturk, "On the performance of artificial bee colony (ABC) algorithm," *Applied Soft Computing*, Vol. 8, No. 1, pp. 687-697, Jan. 2008.
[36] W. Xiang and M. An, "An efficient and robust artificial bee colony algorithm for numerical optimization," *Computers and Operations Research,* Vol. 40, No. 5, pp. 1256-1265, May 2013.
[37] S. Biswas, S. Das, S. Debchoudhury, and S. Kundu, "Coevolving bee colonies by forager migration: A multi-swarm based artificial bee colony algorithm for global search space," *Applied Mathematics and Computation*, Vol. 232, pp. 216-234, Apr. 2014.
[38] A. Ahrari and A. A. Atai, "Grenade explosion method-a novel tool for optimization of multimodal functions," *Applied Soft Computing,* Vol. 10, No. 4, pp. 1132-140, Sep. 2010.
[39] C. Zhang, J. Zheng, and Y. Zhou, "Two modified artificial bee colony algorithms inspired by Grenade explosion method," *Neurocomputing*, Vol. 151, No. 3, pp. 1198-1207, Mar. 2015.
[40] A. Alizadegan, B. Asady, and M. Ahmadpour, "Two modified versions of artificial bee colony algorithm," *Applied Mathematics and Computation*, Vol. 225, pp. 601-609, Dec. 2013.
[41] P. Mansouri, B. Asady, and N. Gupta, "The Bisection–artificial bee colony algorithm to solve fixed point problems," *Applied Soft Computing*, Vol. 26 pp. 143-148, Jan. 2015.
[42] C. H. Lin, "Hybrid recurrent wavelet neural network control of PMSM servo-drive system for electric scooter," *Intl. J. Control, Automation, and Systems,* Vol. 12, No. 1, pp. 77-187, Feb. 2014.
[43] C. H. Lin, "A PMSM driven electric scooter system with V-belt continuously variable transmission using novel hybrid modified recurrent Legendre neural network control," *Journal of Power Electronics*, Vol. 14, No. 5, pp. 1008-1027, Sep. 2014.
[44] C. H. Lin, "Dynamic control of V-belt continuously variable transmission driven electric scooter using hybrid modified recurrent Legendre neural network control system," *Nonlinear Dynamics*, Vol. 79, pp. 787-808, Sep. 2015.
[45] C. H. Lin, "Application of V-belt continuously variable transmission system using hybrid recurrent Laguerre orthogonal polynomials NN control system and modified particle swarm optimization," *J. Computational and Nonlinear Dynamics-Transactions of the ASME*, Vol. 10, No. 5, 16 pages, Sep. 2015.
[46] K. J. Astrom, T. Hagglund, *PID Controller: Theory, Design, and Tuning*, Instrument Society of America, Research Triangle Park, North Carolina, USA, 1995.
[47] T. Hagglund, K. J. Astrom, "Revisiting the Ziegler-Nichols tuning rules for PI control," *Asian J. Control*, Vol. 4, No. 4, pp. 364-380, Dec. 2002.

[48] T. Hagglund and K. J. Astrom, "Revisiting the Ziegler-Nichols tuning rules for PI control-part II: the frequency response method," *Asian J. Contro*l, Vol. 6, No. 4, pp. 469-482, Dec. 2004.
[49] J. J. E. Slotine and W. Li, *Applied Nonlinear Control*, Prentice Hall, Englewood Cliffs, New Jersey, USA, 1991.
[50] K. J. Astrom and B. Wittenmark, *Adaptive Control*, Addison-Wesley, New York, USA, 1995.

Chih-Hong Lin was born in Taichung, Taiwan. He received his B.S. and M.S. degrees in Electrical Engineering from the National Taiwan University of Science and Technology, Taipei, Taiwan, ROC, in 1989 and 1991, respectively. He received his Ph.D. degree in Electrical Engineering from the Chung Yuan Christian University, Zhongli, Taiwan, ROC, in 2001. He is presently working as an Associate Professor in the Department of Electrical Engineering, National United University, Miaoli, Taiwan, ROC. His current research interests include power electronics, motor servo drives and intelligent control.